FLUORIDE CRYSTALS FABRICATION AND PROCESSING – APPLICABILITY AND OPTO-MECHANICAL CHARACTERISTICS

Svilen M. Gechev[1, *], Jordan T. Mouhovski[1], Petar Tzvetkov[2]

[1] Institute of Mineralogy and Crystallography – Bulgarian Academy of Sciences,
Acad. Georgi Bonchev str, bl. 107, 1113 Sofia, Bulgaria

[2] Institute of General and Inorganic Chemistry – Bulgarian Academy of Sciences,
Acad. Georgi Bonchev str. bl.11, 1113 Sofia, Bulgaria

Abstract

Aim of the current survey is a tracking of the crystal growth and further technologically delicate processing in the producing of optical fluoride crystal ingredients. The (doped) fluoride (mono)crystals are attractive to cutting-edge optical/laser/sensor applications. Otherwise, they are not available as high-quality manufactured crystals by conventional or simple growing methods. So, it is required a versatile approach combining or modifying more than one crystal growing technique. It is looked at the optical fluoride (mono)crystals as promising structures for achievement of bigger microelectronic component integration through their use in the future VUV microlithography designing systems or epitaxial layering, etc. By originally modified Bridgman-Stockbarger growing method, there were produced co-doped single and mixed alkaline earth metal fluoride crystals intended to laser issues and application. It was experimentally determined the mechanical quality, optical birefringence and internal stress of such grown crystals and laser optical components finished from them.

Key words: *opto-mechanical uniformity, polariscope/polarimeter, optical fluoride crystals processing, combined Bridgman-Stockbarger method, crystal growth and design*

1. INTRODUCTION

The alkaline earth metal (AEM) fluoride crystals of the type MF_2, where M = Ca, Sr or Ba, or their mixed crystal systems (of the type $M_{1-x}M'_xF_2$ or $M_{1-x-y}M'_xM''_yF_2$, where $M \neq M' \neq M''$) are attractive to optical applications. The use of synthetic optical crystals is essential when the demanded accuracy and the used electromagnetic radiation move beyond the visible spectrum (VIS: 390 – 770 nm) to the ultraviolet (UV) or infrared (IR) ones, respectively.

Among the optical crystal fluorides, CaF_2 is the most typically used compared to crystals as MgF_2 or LiF. The cubic AEM fluoride crystals express high order of crystal symmetry, which supposes a low level of structural defects, while the thermal conductivity is fairly good (~ 10 W/m.K) [*J. Boudeile et al. 2008*]. It is available production of optical fluoride crystals with diameters typically up to 60 cm [*Jordan Mouhovski 2012*]. Compared to glasses and oxide crystals, the optical fluorides also reveal extremely broad optical transmission region from the vacuum UV (VUV) to the near-IR (NIR) range. All those advantages lead to lowering the non-linear optical effects during intensive overall laser radiations.

The above expressed peculiarities combined with the very flat curve of a low-dispersive refractive index and the insignificant birefringence, altogether place the fluoride crystals among the top graded optical/laser materials. Other their excellent properties are the high dispersive power and low chromatic aberrations, and weak luminescence in case of negligible amount of rare-earth element (REE) impurities. Optical isotropy, accurate cleavability, hard resistance under intensive radiations, moderate Raman gain and availability from natural sources as mineral deposited fluorite ores – complete the set of emergency premises about the recent interest in the optical alkaline earth fluoride crystals [*Gechev, S., J. Mouhovski 2013a, b*].

It could be also expressed that the optical AEM fluoride crystals possess some disadvantages – many crystallographic cleavable directions (totally seven for CaF_2); proper structural defects arising in point,

spot, linear or bulk dislocations, fragile fractures or cavities [*Patel A. R. and C. C. Desai 1970*]. Besides also that, REE impurities dominantly in their lower valence states tend to form solid solutions with CaF_2 and the other AEM fluorides. The last leads to increasing the refractive index. Besides the alkaline earth metal fluorides are anisotropic about their mechanical strength and micro-hardness which consecutively increase in the order of the crystallographic directions [111] – [011] – [001] [*Ivanov A. V. et al. 1984*]. There is also anisotropy of the elastic modulus of CaF_2 in different crystallographic planes – maximal on (001) and minimal on (111) [*Jordan Mouhovski 2012*]. In case the structural defects and the chemical impurities are located on the octahedron's edges in the cubic fluorite crystal lattice, they give rise to appearance of selective light dispersive centers [*Muhina T. I. i A. I. Kolyadin 1973*]. Point defects of the sort of vacancies or interstitial ions provoke changes in the fluoride lattice because of the interatomic forces and interactions causing occasional deformations. The proper and/or impurity defects import noticeable changes in the temperature and electric fluoride lattice conductivities.

Strontium fluoride besides as an alternative to CaF_2 takes place as well in several mixed types of fluoride matrixes, e.g. $Ca_{1-x}Sr_xF_2$ wherein Sr^{2+} ions significantly improve the mechanical strength and their larger ionic radii would improve the admixture components segregation coefficient.

The crystal CaF_2 definitely appears the optical medium for the 193-nm and particularly for the 157-nm microlithography projection optics UV-grade. It has significantly better optical characteristics than the commonly used quartz. The microchip industry requires the crystal CaF_2 as microlithography optical projection medium to attain birefringence level less than 1 nm/cm and uniformity better than 1 ppm [*Hand Aaron 2002*]. The theoretical birefringence of the crystal CaF_2 in the far VUV (DUV) range has been calculated to be 18 nm/cm at λ = 157 nm, whereas that 11.8 nm/cm has been measured experimentally [*Burnett J. H. at al 2001*; *Burnett J. et al. 2002*]. Such birefringence values are unacceptably high compared to the desired industrial tolerances of 0.5 – 1 nm/cm. In order of prevention of serious beam bifurcations and phase distortions of the propagating optical wavefronts, there is required appropriate catadioptric compensations in the used stepped lenses of lithography optical cascade systems. If the last is not applied, the VUV microlithography inevitably would lead to blurred imaging [Hand Aaron 2002]. From such point of view, it is impossible the intrinsic birefringence's reduction by attempts of further increase in the single CaF_2 crystals quality. By this reason, it has been developed variety of expensive and sophisticated techniques for adjustment of the microlithography optical cascade systems. In this way, one promising approach could be the experimentally determined opposite signs of the internal birefringence of the single members in some mixed binary fluoride crystal systems such as $CaF_2 – BaF_2$ or $CaF_2 – SrF_2$.

The end members CaF_2 and SrF_2 have been preferred in the earlier stage of the optical and laser-crystal investigations while BaF_2 joined them after repeated optimization process in artificial crystal growth until it finally reached the required optical quality [*Meyer-Fredholm M. M. L. and M. A. Pell 2007*].

In the last decade, the optical AEM fluoride crystals appropriately doped with lanthanides (Ln) and co-doped with transition metals (TM) or alkali metals (AM) are subject of interest in nonlinear optical applications and generation of ultra-short laser pulses in femtosecond domain. Such quantum amplifying media possess relatively broad emission spectra, quite not typical for high ordered crystal structures [*F. Druon et al. 2011*; *Frédéric Druon et al. 2011*]. The near-IR luminescence properties of Yb^{3+}-doped fluoride crystal matrixes are so far not well known. The yellow-green (535 – 560 nm) fluorescence of the Yb^{2+} ions in doped fluoride matrixes is an option for development of novel femtosecond laser amplifiers. Another possible generation of useful laser emissions is through non-parametric processes such as the Stokes and anti-Stokes interactions in the UV – VIS region. Such non-sinusoidal light could be exclusively generated by variations of $\chi^{(3)}$ non-linear laser-lasing doped hosts as the optical fluoride crystal matrixes which can be easily pumped with laser diodes or other powerful coherent sources. The lasant properties of such gained media should be attractive because of the adequate wide spectra they emit during long emission lifetimes. Appropriate mechanism for charge compensation in such hetero-junction isomorphic crystal lattice replacements in structures like e.g. Yb^{3+}:CaF_2 has been proved being the co-doping with Na^+ (NaF) or Li^+ (LiF) [*Burnett J. et al. 2002*].

There is even more lack of comprehensive information concerning the additional influence of monovalent ions such as Li^+ or Na^+ to the absorption and irradiating spectra of Ln-doped optical cubic fluorides.

2. MATERIALS, METHODS AND TECHNOLOGIES

2.1. Crystal growth and design of optical fluorides

Being ionic compounds in their nature, the fluoride crystals are available for crystal growing by several principally different technics: opposite diffusion, hydrothermal growth and from ionic melts. The withdrawal of crystallized fluoride melts expresses definite advantages compared to the others growing technics. Despite, the optical fluoride crystals can be grown successfully by either Czochralski's or Nakkin-Kiropoulos's technics, only Temperature Gradient Techniques (TGT) and Vertical Bridgman (VB) have been recognized being relevant for industrial production of different grades high-quality crystals.

It is essential to underline that *Stockbarger* [*1949 a, b*] was the first researcher succeeded to improve rapidly the traditional Bridgman method. In the search of viable optimization of the thermal conditions into the growing chamber, he replaced the single-zoned Bridgman furnace with such consisted of two zones with independently controlled temperature. The main difference of so called Bridgman-Stockbarger (BS) method compared to Bridgman one, was the existence of separating diaphragm (SD) in the furnace unit between the hot (upper) zone, where the melt is constituted and a low ("cold") zone, where the melt turns into crystal. The SD, in case being significant wide, differentiates intermediate adiabatic zone (AdZ) wherein the undesirable radial inhomogeneities of the thermal field should be minimized. Thus, along the height of the AdZ, the crystallization front (CF) is thought to shift insignificant keeping near to planar form of its curvature. At the same time the construction of the SD should provide for sufficiently steep vertical (axial) temperature gradient that to reduce the probability for appearance of supercooling phenomenon during the melt crystallization. The supercooling effects are a result of impurity segregating processes during the slow and time-consuming growing procedures at crucible's withdrawal toward the cold furnace zone. Disruption of the maximum partial impurity's equidistant concentration is the main reason and criterion for breakage of the normal crystal growth. Such kinds of discontinuity in the layer-by-layer ionic lattice structural crystallization leads to fast stochastic polycrystalization expressed in dendritic and silk-like structures or streak polycrystal forms.

Alternatively to the growing in vacuum or in an inert static atmosphere at pressure over 1 bar, the current BS-crystallization process was done in regime of argon gas flow keeping quasi-equilibrium pressure (≈ 1 mbar) inside the chamber. By essence, it is a modern approach believed to access lower birefringence level of such growing optical AEM fluoride crystals [*Jordan Mouhovski 2012*].

There are many stoichiometric peculiarities how one can ensure optimal crystallization conditions according to the type of the used Bridgman-Stockbarger crystal growing system. As being proved, doping CaF_2 with > 0.2 at.% Yb leads to cluster formation during crystallization [*Andreas Lyberis et al. 2012*] as that undesirable process can be suppressed by introducing an excessive amount of Na ions, tending to clusters' quenching [*L. B. Su et al. 2005*].

Based on variety of prerequisite states, we succeeded to accomplish simultaneous growth of four co-doped crystal boules with two different stoichiometric composition of the matrix: 1.8%(YbF_3),2.5%(NaF):$Ca_{0.67}Sr_{0.33}F_2$ and 1.8%(YbF_3),2.5%(NaF):CaF_2.

The crystal growing was performed by using Bridgman-Stockbarger Growth System – an installation being tailor-made by CRYSTALOX Co., in UK. Both cases of single and mixed AEM fluoride matrixes, it was used sub-millimeter grained natural fluorspar prepared using natural fluorite mined from the mineral deposit Slavyanka (Southwestern Bulgaria). The fluorite pieces (with proven optical quality [*Zidarova, B. 1992*; *Zidarova, B. P. 1995*; *Zidarova, B. P. et al. 1992*]) were subjected consecutively to thermo-breakdown, thermo-shock and sieving, followed by chemical treatment so that the grained substance to attain purity not less than 99.4%. Thus prepared grained material

contained several oxide impurities of Si, Al and Fe, as well as traces of Pb, Mg, Mn, Be, Cu, Sr, Y and REEs [*Zidarova, B. P. 1995*]. In the artificial fluoride crystal growth the usage of natural fluorite instead of synthetic one is preferred owing to lower content of oxygen contaminants and their much easier removing from the grained surface area. Here, an original high temperature procedure was developed to transform the grained stock to several precursors in practical free from molecular oxygen and water vapour [*Jordan Mouhovski 2012*; *Mouchovski J. T. 2007*]. Nearly the same results gave a low-temperature annealing of the starting fluorides mixtures (highly purified fluorspar grains combined with synthetic powders of the rest strontium, ytterbium and sodium fluorides, (Merck, Suprapur), accomplished in advance on 500^{o}C for 20 min under high vacuum.

The crystal growth of both systems (by two mixtures of each type) was carried out simultaneously in the BSGS, the SD of which determines 24.7 mm broad adiabatic zone (AdZ). Since the direct observation of the CF is impossible when using the BS-methods, it was applied an original developed procédure called Quenched Interface in a Multi-cameral graphite Crucible (QIMC) [*Mouchovski J. T. 2007*]. This technique, preceding the real growing, despite being time-consumable, serves successfully for fairly good estimation of optimal crystallization isothermal position within the T-furnace field that should ensure the best quality of the grown crystal boules.

Since the REEs and some others impurities in the used natural fluorite should change unpredictably its m. p. it appeared imperative to be checked the well-known compositional phase diagram of the $Ca_{1-x}Sr_xF_2$ solid solution system via independently performed Differential Thermal Analysis (DTA). All the DTA analyzing had The target was to predefine the optimum melting/crystallizing points for the specific chosen mixed fluoride matrix. Admittedly, the DTA results were compared to other authors' results [*D. Klimm et al. 2008*; *Weller P. F. et al. 1965*]. In general, it was determined the optimum crystallization front position for all solid solutions $Ca_{1-x}Sr_xF_2$ in the range $0 \leq x \leq 1$.

The loaded in crucible inserts starting fluoride portions were mixed thoroughly with 1.5 wt.% PbF_2 as a scavenger to prevent the hydrolytic processes before melting. Thus, PbF_2 produces easily volatile lead oxides thus helping on easily O^{2-} and OH^- desorption from grains-powders particles before their conversion to homogeneous liquid phase [*J. T. Mouchovski et al. 1996*]. Besides by appropriately configured gas-permeability openings drilled axially in the crucibles' lids one may put under control the mass-transport phenomena (predominant Knudsen diffusion) and materials sublimation during the whole growing process [*J. T. Mouchovski et al. 1996*]. After the high-temperature treatment of so prepared mixtures being performed, the produce highly purified precursors were loaded re-loaded in the relevant crucible inserts and the real crystal growth experiment was carried out in a regime of dynamical quasi-constant flow of argon gas (> 99.99% purity) at sub-atmospheric pressure ranged within 5 – 7 mbar. The experiment duration was about three nights and days, finishing with total annealing prolongation of ~28 h, the last 12 h of them dedicated to some finer annealing.

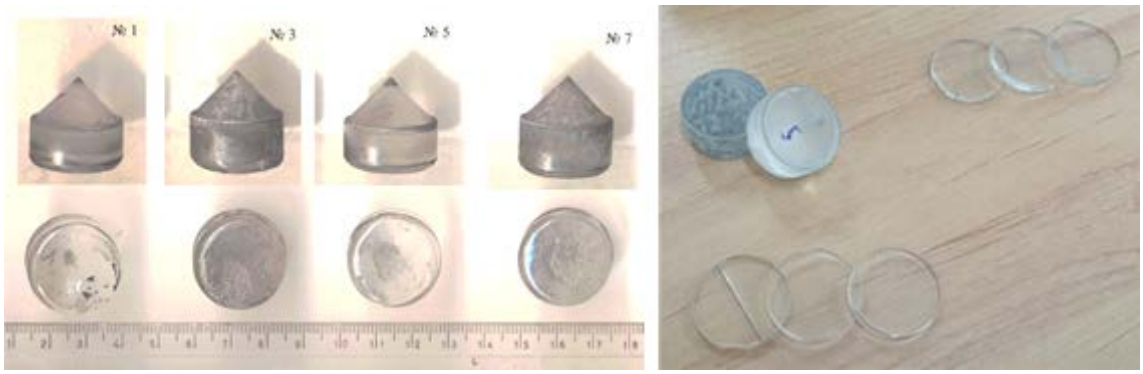


Figure 1. On the left: crystal boules with different content grown by modified vertical BS method: 1 and 5 – 1.8%(YbF_3),2.5%(NaF):$Ca_{0.67}Sr_{0.33}F_2$; 3 and 7 – 1.8%(YbF_3),2.5%(NaF):CaF_2; On the right: finished optical windows (each with dimensions 1" in diameter × 2.9 mm ± 0.1 mm) from the boules №: 1 (down) and 7 respectively (upper).

The crystallization process runs in a graphite multi-cameral crucible consisting of finely carved sockets (nests) – one single central (with diameter 2"), surrounded by eight other peripheral axial-symmetrically located ones. The relevant inserts loaded with the mixtures were put inside four of the eight peripheral nests, symmetrically sited (2 × 2 diametrically opposed on a cross). The inserts were with equal height, having internal diameter of 1" and walls' thickness of 2.8 mm as their bottoms are oblique under angle of 90º for viable initiation of crystal nucleation. The lids of the individual inserts were with thicknesses of 2.5 or 3 mm, and they had by one differently sized centrally drilled small round hole (channel).

The successfully grown fluoride crystals exhibit ideally shaped conical bottoms (directed upward in Fig. 1 upper on the left). This fact manifests normal growth conditions being attained, a result of single spontaneous nucleation center located in the very conical tips of each crucible's insert.

The dark coloration of the crystals' surfaces is due to firmly adhered polyp crusts combined with finely dispersed graphite particles. The bottom tipped crucible inserts' construction determines the type and the distribution of the crystal boules' crusts. This phenomenon appears as a result of fluoride species' condensation on the crystals' surfaces. It occurs in miniature peripheral cavities formed between the growing crystal and the surrounding graphite walls. The micro-cavities are caused by the effect of the reflected thermal radiation from the smooth bottoms of the graphite inserts. In this way, it has been simultaneously modified the coefficient of thermal expansion of the fluoride crystals and the graphite inserts along their vertical lengths [*J. Mouhovski et al. 2014*].

The rear (upper bottom) surfaces of the produced crystals are slightly curved along their peripheral edges. Otherwise in their bottom planes they are "flat" but with some areas with very minor rough deviations, smaller than a millimeter. The minor rough deviations are likely due to some radial inhomogeneity of the temperature (T-) field during the final stage of the boules' growing whereat the real growth rate becomes increasingly higher than the speed of crucible withdrawal. Besides, it is possible to be sealed impurities concentrations in certain areas, and a formation of coating structures or rough scabs due to the effects of sublimation/condensation of fluoride particles and impurities (contaminants) on the bottom crystal surfaces. It is noticeable that all figured out effects are mainly distinguishable for the boules denoted by 3 and 7 (the crystal system 1.8%(YbF_3),2.5%(NaF):CaF_2). These crystal boules are coated with dark polyp crusts while the boules denoted as 1 and 5 (the crystal system 1.8%(YbF_3),2.5%(NaF):$Ca_{0.67}Sr_{0.33}F_2$) have, in general, no deposited surface polyp crusts. The later manifests more uniform residual partial pressures established into the cavity between the growing boules and the inserts' walls. Under the crusts adhered to the crystals' walls, all the boules appear visible transparent.

2.2. Optical fluoride crystals processing

2.2.1. Crystallographic orientation

The boules of the investigated crystal systems were grown simultaneously under identical conditions with insignificant deviation of the crystallographic direction (111), recognized this corresponding to superior octahedral cleavage of the cubic AEM fluoride crystals. The deviations from the ideal crystallographic plane (111) were determined being in the order of hundredths of a degree. For precise orientation analysis it was used X-ray powder diffractometer BRUKER D8 ADVANCE in regime of φ-scan X-ray technique, Ni-filtered with radiation Cu Kα line λ = 0.154060 nm and in parallel geometry. The optical CaF_2 has lowest internal birefringence right over the crystallographic plane (111). On the other hand, the planes in direction (001) are considered as the most appropriate for fluorescent (luminescent) arising and other absorbing/emitting laser issues, while in the crystallographic planes of (110) the optical CaF_2 has the best mechanical hardness [*Jordan Mouhovski 2012*].

2.2.2. Manufacturing of optical fluoride crystal ingredients

They were chosen the crystal boules numbered as 1 and 7, i.e. by one boule from each type of the crystal systems, therefrom were prepared by three neighbor optical windows. The cutting process was ensured by thin filament (with thickness 0.2 mm), lavishly wet with water or heat-removing liquids. At typical cutting rates of 0.5 – 1 cm/h, they were cut the conical sections from the boules. By the same manner from the cylindrical boules' sections, they were cut in parallel separate circular disks, one over another from which were finished relevant optical windows, each with dimensions of (1" × 3.0) ± 0.1 mm. For clearance, the disks were denoted by: 1 – 1, 1 – 2, 1 – 3 and respectively 7 – 1, 7 – 2, 7 – 3. Here, the first index indicates the number of the crystal boule (and that is also the type of the crystal system), while the second – shows the number of the consecutively cutting disk, starting from the bottom conical section of the boules. Each optical disk was slightly sloped from the ideal circular aperture and across the peripheral sloped wall was numbered by the mentioned nomenclature designation. In the production process, because of the fluorides friability and the many axes of cleavability, it was imperative many times fine polishing of the optical disks so they become of final thicknesses as optical windows of (2.9 ± 0.1) mm.

The optical CaF_2 crystals processing, generally includes the technological operations of crystallographic orientation, cutting, grinding, polishing and fine polish treatment. Their full automation is difficult for achieving because the crystal fluoride materials are characterized with relatively low level of hardness and sometimes sharply manifested mechanical anisotropy, let assume as well not high heat resistance threshold and the cleaving tendencies over different cutting planes. Therefore, it is acceptable the manual or semi-automatic fluoride crystals processing [*Optical Crystals by Optovac 1982*], combined with samples' blocking (sticking), together following the presumption for equal surface treatments.

For tuning-up the grinding process, it can be used a surface activator on the basis of dilute solutions of hydrochloric or nitric acids. The activators have to be applied simultaneously to the main grinding treatments which are typically carried out with diamond pastes and powders. Using surface activator, the accuracy improves significantly and any local errors are drastically reducible. Here, in the current grinding processing, it was used polyurethane film coated with abrasive resin, which was blurry applied on the optical discs and the used four different grinding machines.

The CaF_2 micro-hardness by the Mohs' scale is 4.0. This value is significantly lower than that of the ordinary glasses (> 5.0). This hampers the fine optical fluorides' polishing and micro-grains or particles often are ripped off from the threated surface of the crystal fluorides. CaF_2 is practically insoluble in water and under normal atmospheric conditions and sustains optical polishing without ageing deterioration of the crystal quality or those processes are reversible after surface cleaning. The material exhibits inertness to the most chemical compounds, but is assailable from aggressive acids. Practically the crystal CaF_2 has no plasticity in its nature and possesses non-variable universal refractive index and dispersive values, i.e. the crystal AEM fluorides in fact have no the so called group-dispersive velocity characteristics as the glasses.

Fluoride crystals cuttings over the cleavage planes are not recommended, since this could lead to bursting. Perhaps that is the reason, the manufacturing of the first (lowest located) optical window, labeled as 1 – 1, to show radial partial structural defect along its diameter. In subsequent treatment procedures the crystal disk appeared divided into two relatively equal in diameter halves. Surprisingly, this fact does not correspond to the expected improvement of the mechanical strength of the grown boules, the Sr content in which system (more than 30 wt.%), presupposes some improvement of crystal mechanical strength.

2.2.3. Specificity in fluorides grinding and fine polishing

For polishing the optical fluoride disks of the systems 1.8%(YbF_3),2.5%(NaF):$Ca_{0.67}Sr_{0.33}F_2$ and 1.8%(YbF_3),2.5%(NaF):CaF_2, it was used consecutively abrasive pastes of vanadium carbide with grain sizes respectively 6, 3 and 1 μm. The fine polishing was performed consecutively by using two pure alundum pastes with particle sizes of 0.28 μm (treatment for about 1 h) and 0.2 μm (treatment for about 20 min), respectively

The successful optical fluoride crystals processing is a matter of the materials sensitivity to mechanical and thermal shocks. Excessive shocks cause cleavage mostly over (111), which in the present study is the plane, in parallel of which we did the crystals cutting issue. As a matter of fact this appeared a huge advantage and lowered the significant risk of possible crystal cleavage.

Finished optical fluoride windows should be stored in dry places (best in desiccators), because over the time their surfaces adsorb moisture and hydrocarbons from the ambient atmosphere. That leads not only to integral deterioration of the spectral transmission characteristics, but also to the emergence of specific IR-adsorption hydrocarbon bands.

The minimum quality demands for optical windows/flat mirrors of CaF_2 for VUV – UV region are: surface figuring (on both surfaces) not more than 1 – 2 wavelengths upon irradiation of 632.8 nm (emitted by He – Ne laser); surface polishing (on both surfaces) max. 20 – 10 dug scratches; plane-parallelism typically ≤ 3 arc minutes (UV) or ≤ 10 arc seconds (VUV) [*High Power Excimer & UV Laser Optics 1986*].

2.3. Optical birefringence of fluoride crystals

The cubic lattice symmetry of the AEM fluorides crystals provides, as a whole, isotropy of their optical properties, such as absorbance, refractive index, and e.t.c. However, as noted firstly by Lorentz even before J. C. Maxwell to formulate the macroscopic electromagnetic equations, the optical cubic crystals isotropy impairs over propagation of the short-wavelength light (e.g. in the VUV range). This is due to symmetry break because limitation in the values of the wave vector of light, which results in inherent materials birefringence [*H. A. Lorentz 1878, 1921*]. This effect is known as internal birefringence caused by spatial dispersion.

The values of the intrinsic birefringence for CaF_2 are lower than $\Delta n = 1 \times 10^{-7}$ at $\lambda = 365$ nm (UV range) but they increase significantly at shorter wavelengths in accordance with the relationship:

$$\Delta n \approx 1/\lambda^2\left(q^2\right) \quad (1),$$

where: λ is the wavelength and q – the value (direction) of the wave vector [*John H. Burnett et al. 2001*].

Equation (1) explains why the effect of internal birefringence is not tangible for larger wavelengths in optical materials. Shorter wavelengths produce high spatial dispersion, which excludes low intrinsic birefringence values and, for example, they are much higher than the values of the additional dispersion induced by the piezo-optical effect in CaF_2 or that in BaF_2 [*J. H. Burnett 2000*]. The internal birefringence in CaF_2 at 193 and especially at 157 nm is very high, compared to cited values of 1×10^{-7} demanded for the needs of VUV microlithography (starting-down at 157 nm) [*A. K. Bates 2000*].

The precision UV lenses of CaF_2 for the practice are usually oriented in crystallographic directions [111] or [100] taking into account the viewpoint of the falling electromagnetic field distribution. About round lenses with a given numerical aperture (NA), only matter has the change in the refractive index through the waves' propagation under certain angles. Practically, there is no birefringence upon propagation exactly over the axis of directions [111] or [100] and that is believed it is true also for small angles in close vicinity to both these directions. Thus, the birefringence effect can be avoided for small NA [*J. H. Burnett 2000*], but not for high numerical aperture values, used for example, in the micro-photolithography systems. Maximum effect of the internal birefringence could be realized for the waves falling into the crystal of AEM fluoride substance in directions at angles of $\cos^{-1}[(2/3)^{1/2}] \approx 35.26$ (or at 45°) [*J. H. Burnett 2000*]. It should be also noted that the birefringence least depends from the angle's deviation of the wave propagation in the environment vicinity close to [100] rather than to propagation in direction [111]. This is related to the extreme minimum birefringence value in the direction of propagation [100] in the crystal CaF_2 and leads to an advantage of such lenses in which the beams propagate over just optical direction [100].

The theoretically and experimentally determined intrinsic birefringence in cubic crystalline optical designated systems is large enough to cause serious consequences in the overall accuracy of the modern UV optical technologies. Nevertheless, the symmetry of this phenomenon may provide a solution to the problem. Optical elements, oriented for ray propagation over the optical axis [111] or [100], combined with other optical elements, oriented transversally to the first elements' crystal axis, bring out relative beam rotation at 60° (or at 45°), and thus totally provide an effect of partial internal birefringence compensation [*J. H. Burnett 2000*]. Otherwise, in the attempts for simplifying all these complicated and cost consuming techniques, it could be applied the technological solution based on the reverse birefringence signs of the CaF_2 crystals versus the BaF_2 or SrF_2 crystals. The combination provides the desired birefringence compensation. Moreover, the growth of mixed fluoride crystal systems of the type of $Ca_{1-x}Sr_xF_2$ could completely remove the influence of the internal birefringence for a given wavelength or even frequency range.

Except the internal birefringence inherent for a given material in the real artificial crystal growing processes or through the crystals formation under natural conditions, there inevitably act different thermal, mechanical and other tensions, which affect the ideal structural crystal lattice arrangement. The modern micro-lithography requires a maximum of about 1 nm/cm ($\Delta n \approx 1 \times 10^{-6}$ at 157 nm) difference in the beams' paths between the ordinary and the extraordinary waves after mechanically induced birefringence throughout the CaF_2 crystals intended for usage at the border between DUV and VUV. This value appears almost of an order of magnitude higher than that of the typical internal birefringence of CaF_2 at DUV/VUV border. The best experimentally measured birefringence values engendered of opto-mechanical anisotropy in crystal CaF_2 are, so far, of two orders of magnitude higher than those measured for the proper intrinsic birefringence of the same material [*Burnett J. et al. 2002*; *John H. Burnett et al. 2001*].

2.4. Polariscopy (polarimetry)

For determination of the total birefringence (internal + mechanically induced) it was used polariscope/polarimeter PKS-250 U.4.1 produced in Russia. This device is most suitable for analyzing the flat or finely polished transparent or pale samples, operating in two different modes:

- Approximate estimation of the sample's birefringence observing the coloration of interference pattern.
- Quantitative assessment of the optical paths difference bred through the propagation of the ordinary and extraordinary rays in a given sample.

The extended threshold limit in the assessment of the optical beam paths difference in PKS-250 U.4.1, (using λ/4 plate) is one wavelength. The measuring error using Senarmont's compensator (i.e. polarimetric mode) is ± 10 nm. PKS-250 U.4.1 is also equipped with internal lamp source of 500 W, the light of which is filtered to transmit a monochromatic beam at 540 nm.

Shady semi-darkling conditions appear most effective for device operation, accomplishing by diffusive scattered radiation. The beam from the internal light source passes through optical lens system, being then redirected to a polarizer and after that – to λ- or λ/4-thick optical plate. Finally, such obtained light signal attains to a rotating matte glass on which it has been placed the test sample. Propagating through the sample, the polarized light undergoes the birefringence effect as the directions of the electromagnetic oscillator vectors of the ordinary and extraordinary waves are orthogonal and their vibrations are phase-shifted depending on the induced mechanical stress in the sample and the ran optical path through it. Optical analyzer shows the birefringence difference in one plane as colored interference pattern for each point of sample's bulk.

In PKS-250 U.4.1, the λ-thick plate results in distance difference of 572 nm in the rays' propagated ways. The λ-thick plate is located in a manner that the directions of the fast oscillations in it conclude an angle of 45º with the polarizer's electric vector oscillation direction. The studied sample is usually placed so to reveal a purple-violet coloration corresponding to zero birefringence (Table 1). Minor changes in the beam path (± 12 – 15 nm) by rotating the sample or the polarizer lead to relevant

change in coloration. The difference in the optical paths owing to optical heterogeneity can be expressed by:

$$\Gamma[nm] = (n_1 - n_2) \cdot L \quad (2),$$

where: n_1 and n_2 are the refractive indexes respectively of the ordinary and the extraordinary rays; L is a sample's thickness.

Interference coloration	*Wavelenght, λ [nm]*	*Interference coloration*	*Wavelenght, λ [nm]*
Yellow	325	Red	25
Yellow-green	275	Orange	130
Green	200	Light yellow	200
Blue-green	145	Yellow	260
Blue	115	White	310
Purple-violet	0		

Table 1. Interference coloration scale, corresponding to birefringence level, when using PKS-250 U.4.1 device in polariscopic mode.

The magnitude Γ defines the dependence of the interference coloration total birefringence. In this case, PKS-250 U.4.1 operates in polariscopic mode.

The λ/4 plate can be mechanically replaced by λ-plate in the optical system, when it is needed quantitative birefringence assessment. This way PKS-250 U.4.1 moves on polarimetric mode. The λ-plate's action lies on the elliptical polarized beam transformation from the studied sample to linearly polarized beam. The sample is placed in the center of the rotating matte glass and the studied area has to be darkened. When the matte glass is scaling rotated at 45º, the sample appears already enlightened. Then the sample is again maximally darkened by rotating the analyzer with precision Vernier scale (up to 0.1º) equipped with color filter. The difference between the angle on which are being rotated the analyzer and the zero (initial) position of the sample gives the angle θ in Eq. (3) below. In fact, the λ/4-thick optical plate plus the rotating analyzer constitute Senarmont's compensator, this way making the device to operate as polarimeter. The beam path difference, i.e. the magnitude Γ expressing the optical anisotropy of the tested sample, is defined simply by:

$$\Gamma[nm/cm] = 3 \cdot \theta \quad (3).$$

3. RESULTS AND DISCISION

For investigation of relatively small objects it is sufficient to be used the λ-thick optical plate of PKS-250 U.4.1. The polariscopic measurements were performed on all finished optical windows, as in Fig. 2 are given the most representative ones: Nos. 1 – 2 and 1 – 3 [1.8%(YbF_3),2.5%(NaF):$Ca_{0.67}Sr_{0.33}F_2$] as well as Nos. 7 – 2 and 7 – 3 [1.8%(YbF_3),2.5%(NaF):CaF_2].

In Fig. 2 and Fig. 4 are presented consecutively the pictures of polariscopic measurements for several studied optical windows and crystal boules. The polariscopic patterns of optical windows 1 – 2 and 1 – 3 reveal homogeneous purple-violet coloration over their entire cross sections and volumes. Likewise, a thin weak red hue is perceived over their edges. The purple-violet color corresponds to practically lack of optical anisotropy (Table 1). This is an expected result because of the opposite signs (negative for CaF_2 and positive for SrF_2) and the mutual reciprocal compensation of the intrinsic birefringence in the mixed fluoride crystal matrixes $Ca_{0.67}Sr_{0.33}F_2$. The higher mechanical strength of SrF_2 and the considerably larger ionic radius of Sr^{2+} compared to that of Ca^{2+} promote structural defects quenching in the crystal lattice, as a result of which the mechanical stress remains with minimal effect. The reddish thin peripheral hues (Γ = 25 nm) should be caused by edge effects bred by the alternation in the difference between the temperature volume expansion coefficients of growing boules and

supporting them graphite inserts into used multi-cameral crucible. Besides, the red hue at the edges might be caused by some mechanical stresses, typically accompanying the cutting, grinding and polishing operational processes and even likely induced during the mechanical removal of the firmly adhered polyp crusts on the lateral surfaces of the boules. Inevitably, any contacts with exterior bodies and surfaces and the manipulations with tweezers or handy during sample tests and measurements complete the full set of possible reasons for the red hue edging.

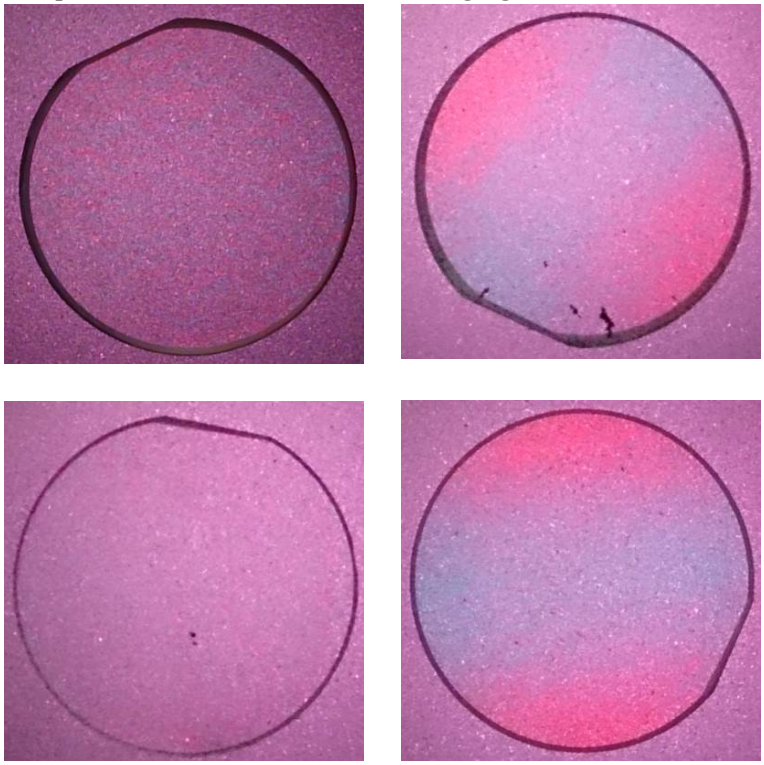


Figure 2. Colorized polariscopic patterns of the finished optical windows. On left: 1 – 2 and 1 – 3 (1.8%(YbF_3),2.5%(NaF):$Ca_{0.67}Sr_{0.33}F_2$); On right: 7 – 2, 7 – 3 (1.8%(YbF_3),2.5%(NaF):CaF_2).

Concerning the crystal system 1.8%(YbF_3),2.5%(NaF):CaF_2 (on the right of Fig. 2), the optical windows 7 – 2 and 7 – 3 present one and the same large central areas with pale light-blue colorations (Γ = 115 nm). These areas capture the middle optical windows sections from edge to edge. For both those optical windows, there are purple-violet peripheral-sided areas away from the wide blue regions in the samples' middles. The presented polariscopic patterns, expressing birefringence in blue coloration, could be well explained with that the stresses in the samples periphery always tend to partially or completely offset each other (purple-violet coloration) but in the central area at least part of the mechanical tensions inevitably remain.

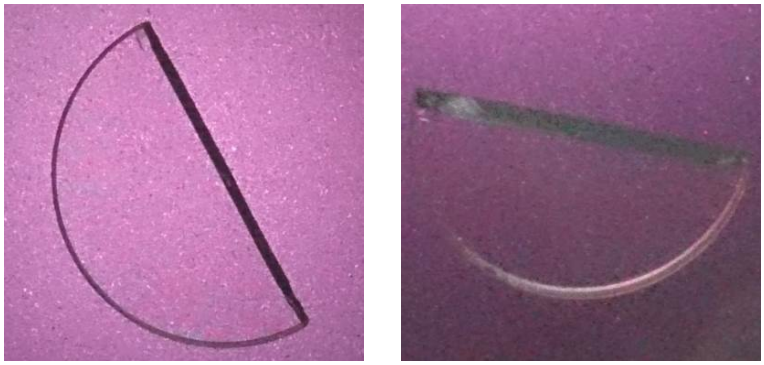


Figure 3. Colorized polariscopic patterns of segmented section of optical window 1 – 1 [1.8%(YbF_3),2.5%(NaF):$Ca_{0.67}Sr_{0.33}F_2$]. On the left: horizontal polariscopic pattern; on the right: the segment's cleavage direction which in this case is angled on 13º to the direction of crystal growth [111].

Because both crystal systems were grown simultaneously and under identical conditions, the occurrence of optical anisotropy in CaF_2-matrix can be attributed to the inherent birefringence and to higher local impurities' concentration causing relevant structural deformation. The opto-mechanical properties are worse for the single crystal fluoride lattice which is more plastic and more movable compared to the lattice of $Ca_{0.67}Sr_{0.33}F_2$. Otherwise, under inverting the polarization directions, i.e. rotation the optical window or the polarizer on 90º – the colorations of the tested samples change completely reciprocal in unison each to other.

In Fig. 3 are shown polariscopic patterns for segmented section of optical window 1 – 1. This window has evidently exhibited diametrically sited partial structural defect during the manufacturing that afterwards spread within the crystal bulk that finally has led to splitting the window on two relatively equal parts. On the left in the figure, it is seen the inherent lack of birefringence expressed by homogeneous purple-violet coloration. There is again a presence of the typical thin weak reddish hue over the optical segment's edge. On the right in Fig. 3, the optical segment is sloped under angle of 13º compared to its cross-section plane which expresses the caused slope of cleavage. The splitting surface characterizes itself by saturated green coloration, which corresponds to 200 nm birefringence between the ordinary and extraordinary wave propagated paths.

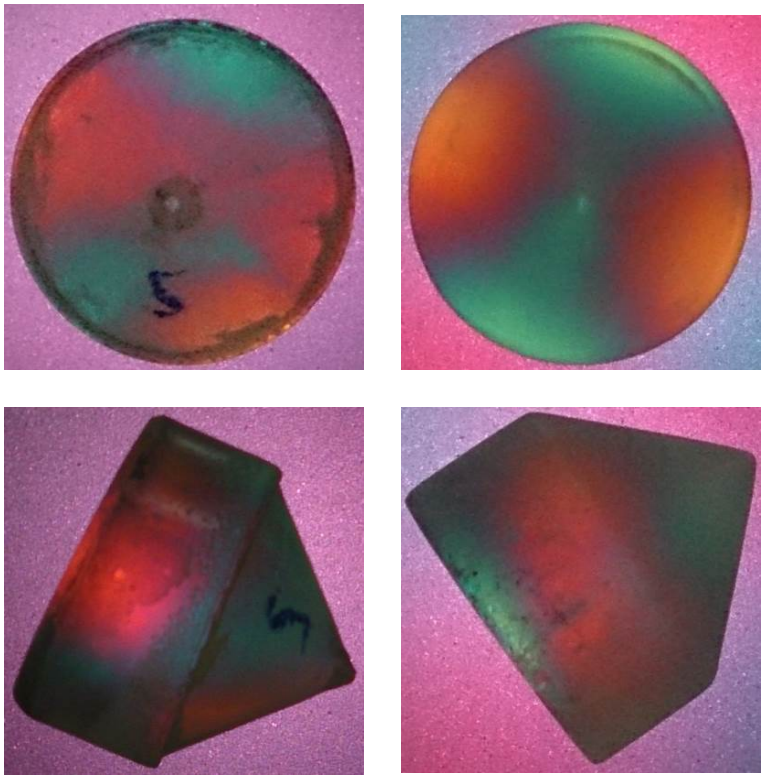


Figure 4. On the left – boule 5 [1.8%(YbF_3),2.5%(NaF):$Ca_{0.67}Sr_{0.33}F_2$], on the right – boule 3 [1.8%(YbF_3),2.5%(NaF):CaF_2]; Upper photos show – an axial view from the top of the conical crystal parts; Lower photos – side view.

Figure 4 presents polariscopic patterns of the boules numbered as 5 and 3, which have the same chemical composition like those numbered as 1 and 7, therefrom were finished both optical windows series. In polariscopic mode, a lateral point of view over the two boules reveals centered bright red

colored interference (Γ = 25 nm). In the vicinities of their flat top surfaces as well as on the lateral sides, and the cone sections, the coloration is green (Γ = 200 nm). The red surface area for boule 5 is smaller being centered in the cylindrical section, while for boule 3 – the area fills the middle and the upper cylindrical section, and also the widest 1/3 part of the cone section. Up on the photos in Fig. 4, the crystal boules were placed with their flat top faces over the polariscope's matte glass surface. The photos were taken ahead the conical tips. As concern the boule 5, its predominant coloration is red and only two green segmented radially-opposite bulk sections appear peripherally located. It could be seen too brownish hues and contaminations caused due to some thin polyps situated on crystal surface. The boules 3 and 7 (matrix of CaF_2) have found to grew-up with firmly surface adhered opaque polyp crusts by contrast with those having matrixes of $Ca_{0.67}Sr_{0.33}F_2$ (boules 1 and 5). To clear the boules with opaque crust adhered onto their lateral and bottom surfaces, we removed completely the crust before using the boules for polariscopic measurements. This is why for the crystal boule 3 on the right in Fig. 4, it is observable fully symmetrical axial viewed interference pattern with predominant green color as well as two deep peripherally-sided segments in orange color.

The polariscopic patterns shown in Fig. 4 reveal significant level of internal stresses in their conical section. This fact could be explained by the presence of more impurities and moisture therein due to not still efficient (self)purged or degassed within the initial stage of the BS crystal growing accompanied with unstable T-field in radial direction during the growth of the cone section. In its middle parts the boules reveal much stable growing behavior and should be mostly free of contaminants, part of which have been sunk in the melts before growing to start, the rest being rejected ahead the CF. At the end of the crystal growing, with finalization of the boules withdrawal (the last 5 – 6 mm of their height) it is again observable structural inhomogeneity caused by the thermal convections existing in the final crystalizing melt. Besides, the impurities' concentrations in this last bulk region should increase significantly thus altering the normal growth to bulk or dendritic ones. Finally, the thermal field outside the AdZ becomes more and more inhomogeneous altering the shape of shifter therein crystallization isotherm and following it CF. The reason for perturbation thermal effects within the whole furnace unit lies mainly in the imperfection of the overall pursuing of the programmed temperature regimes for the upper and lower zones in even modified BS furnace unit.

4. CONCLUSIONS

By using originally modified BS technique and under identical conditions, they are successfully grown co-doped single and mixed AEM fluoride crystals in the form of boules with conical bottom. From two arbitrarily chosen boules, by one of both crystal systems – 1.8%(YbF_3),2.5%(NaF):$Ca_{0.67}Sr_{0.33}F_2$ and 1.8%(YbF_3),2.5%(NaF):CaF_2 are finished series of optical windows.

The residual mechanical stresses in the boules are partly generated because of the stage of rough annealing the just grown boules, which 28 hours duration reduces the internal bulk stresses but not those external ones caused by arising temperature shrinking effect for the already grown boules and the graphite crucible's inserts. Since the pure crystal graphite has a greater volume expansion coefficient than the relevant AEM fluorides crystals, the crucible inserts walls press on the cooling boules. Only during the crystals' cooling around the phase transition from tetragonal to cubic CaF_2 at 1150^{o}C, the graphite crucible's inserts have smaller thermal volumetric expansion than that of the calcium fluoride crystal. At this juncture, the occurrence of mechanical stress effects during the otherwise slow thermal crystals annealing appears inevitable that imposes the further reduction of the internal mechanical lattice tensions being accomplished by implementation of additional fine annealing.

The polariscopic analyses of finished optical windows of the grown boules show only the windows with chemical composition 1.8%(YbF_3),2.5%(NaF):$Ca_{0.67}Sr_{0.33}F_2$ do not suggest in practice residual mechanical stress that to cause significant birefringence effect. Some small local structural-mechanical forces and stresses were found for the other type of studied fluoride crystal system 1.8%(YbF_3),2.5%(NaF):CaF_2. The different behavior of the two systems as concern the birefringence effect is due to peculiarities of their matrix.

That of the type of $Ca_{0.67}Sr_{0.33}F_2$ shows tend to improve the lattice strength as the larger volume of Sr^{2+} can better compensate any external forces and mechanical influences. Otherwise, the perfect crystal structure depends substantially on efficient control of the T-field during the entire growing that can be attained modifying appropriately the construction the BS furnace unit not mounting auxiliary heater(s) but only introducing additional system of molybdenum shields for keeping as long T-homogeneity along the crucible withdrawal as it is necessary to provide normal growth. Besides, a strict control upon the mass-transport processes can be successfully accomplished by varying the ambient composition and using a crucible with special original construction. For less deviation in the T-field in the furnace unit it is recommended implementation of crucible rotation being during the whole growing and following annealing.

ACKNOWLEDGEMENTS

This work was supported by the European Social Fund and Republic of Bulgaria, Operational Programme "Human Resources Development", 2007 – 2013 framework, Grant № BG051PO001-3.3.06-0027 from July 2013.

Special thanks to Opteco & Partners Ltd. and its managing director Dr. Dipl. Eng. Nikola Dimitrov about the optical fluoride crystals processing and the precisely performed technological operations of cutting, grinding and fine polishing.

REFERENCES

A. K. Bates, In: "Proceedings of the First International Symposium on 157 nm Lithography," edited by R. Harbison, *International SEMATECH* (Austin 2000), p. 377.

Andreas Lyberis, Adam J. Stevenson, Akiko Suganuma, Sandrine Ricaud, Frederic Druon, Frederic Herbst, Daniel Vivien, Patrick Gredin, Michel Mortier, "Effect of Yb^{3+} concentration on optical properties of Yb:CaF_2 transparent ceramics," *Optical Materials* (2012), 34, 965 – 968.

Burnett J. H., Z. H. Levine, E. L. Shirley, "Intrinsic birefringence in calcium fluoride and barium fluoride," *Phys. Rev. B* (2001), 64, 241102(R), 1 – 4.

Burnett J. H., Z. H. Levine, E. L. Shirley, "Minimizing Spatial-Dispersion-Induced Birefringence in Crystals for Precision Optics by Using Mixed Crystals of Materials with the Opposite Sign of the Birefringence," *Phys. Lab., Atom. Phys. Div., NIST*, Plasma Radiation Group (dated: March 26, 2002), <http://physics.nist.gov/Divisions/Div842/Gp3/DUVMatChar/birefring.html>, (Online July 12 2001). See also in: "Invention Disclosure," Gaithersburg, MD, USA: *National Institute of Standards and Technology*, pp. 1 – 3.

F. Druon, F. Balembois, P. Georges, "New materials for short-pulse amplifiers (Invited Paper)," *IEEE Photonics Journal "New materials for amplifiers"* (2011), 3, 2, 268 – 273.

Frédéric Druon, Sandrine Ricaud, Dimitris N. Papadopoulos, Alain Pellegrina, Patrice Camy, Jean Louis Doualan, Richard Moncorgé, Antoine Courjaud, Eric Mottay, and Patrick Georges, "On Yb:CaF_2 and Yb:SrF_2: review of spectroscopic and thermal properties and their impact on femtosecond and high power laser performance [Invited]," *Optical Materials Express* (2011), 1, 3, pp. 502.

Gechev, S., J. Mouhovski, "Growth conditions of $Ca_{1-x}Sr_xF_2$ optical monocrystals by Bridgman-Stockbarger method," *VI Spring Seminar for Young Scientists and PhD students of Chemical Institutes of BAS "Interdisciplinary chemistry"* – Abstract and Presentation (Creative House of BAS, Vitosha 2013a).

Gechev, S., J. Mouhovski, "Purification of natural fluorspar for optical crystal growth," – In: *National conference "Geosciences 2013" with international participation* – Poster Session and Proceedings (Sofia, Bulgaria 2013b), 21 – 22.

H. A. Lorentz, "Collected Papers II," (Martinus Nijohff, The Hague, 1936), pp. 1 – 119, esp. p. 79; *Verh. K. Akad. Wet*. Amsterdam, Afd. Natuurkd. (1878), 18.

H. A. Lorentz, "Collected Papers III," (Martinus Nijohff, The Hague, 1936), pp. 314 – 320; *Proc. R. Acad. Sci.* Amsterdam (1921), 24, pp. 333.

Hand Aaron (Man. Ed.). *Semicond. Intern*. (2002), 2/1/02. <www.tf.uni-kiel.de/matwis/amat/elmat_en/kap_6/advanced/t6_6_1.html>

High Power Excimer & UV Laser Optics, "Prospect. Acton Research Corporation," *Prospect*, Acton, Massachusetts (1986), pp. 19.

Ivanov A. V., S. I. Derjavin, V. M. Rejiterov, "Mekhanicheskaya prochnost' kristallov ftoridov kal'tziya i bariya," *Opt. Mekh. Prom*. (1984), 5, 27 – 28 (in Russian).

J. Boudeile, J. Didierjean, P. Camy, J. L. Doualan, A. Benayad, V. Ménard, R. Moncorgé, F. Druon, F. Balembois, and P. Georges, "Thermal behaviour of ytterbium-doped fluorite crystals under high power pumping," *Opt. Express* (2008), 16, 10098 – 10109,

J. H. Burnett, In: "Proceedings of 157 nm Technical Data Review," edited by R. Harbison, *International SEMATECH* (Austin 2000).

J. Mouhovski, O. Vitov, V. Dimov, B. Kostova, S. Gechev, "High vacuum phase transformation of fluorspar vapors to crystal aggregates," *Bulg. Chem. Commun.* (2014), 46, 1, 68 – 78.

Jordan Mouhovski, "Optical fluorides – Purification and crystal growing applicability and perspectives", *Prof. Marin Drinov Academic Publishing House* (Sofia 2012).

J. T. Mouchovski, I. V. Haltakov, V. L. Lyutskanov, "Growth of ultra-violet grade CaF_2 crystals and their application for excimer laser optics," (April 2 1996) 162, 1 – 2, 79 – 82.

Klimm D., M. Rabe, R. Bertram, R. Uecker, L. Parthier, "Phase diagram analysis and crystal growth of solid solutions $Ca_{1-x}Sr_xF_2$," *J. Cryst. Growth* (2008), 310, 1, 152 – 155.

L. B. Su, J. Xu, H. J. Li, W. Q. Yang, Z. W. Zhao, J. L. Si, Y. J. Dong, and G. Q. Zhou, "Codoping Na^+ to modulate the spectroscopy and photoluminescence properties of Yb^{3+} in CaF_2 laser crystal," *Opt. Lett.* (2005), 30, 9, 1003 – 1005.

Meyer-Fredholm M. M. L. and M. A. Pell, "Preparation of 157 nm transmitting barium fluoride crystals with permeable graphite," *US Patent* 7, 276, 219, (Feb 10 2007), Int. Cl.: C01B33/26; C30B13/02; C30B13/04.

Mouchovski J. T., "Control of oxygen contamination during the growth of optical calcium fluoride and calcium strontium fluoride crystals," *Prog. Cryst. Growth Charact. Matter*. (2007), 53, 79 – 116.

Muhina T. I. i A. I. Kolyadin, "Selectivnoe passeyanie sveta v monokristallah ftoristogo kal'tziya," *Opt. Mekh. Prom*. (1973), 3, 28 – 31 (in Russian).

Optical Crystals by Optovac, "Handbook of optics," *Optovac Inc.*, North Brookfield, Massachusetts (1982), 4 – 1, 5 – 3.

Patel A. R. and C. C. Desai, "Effect of impurities on the plastic deformation of calcium fluoride single crystals." *J. Phys. D: Appl. Phys.* (1970), 3, 11, 1645 –1648.

Stockbarger D. C., "Artificial Fluorite," *J. Opt. Soc. Am.* (1949a), 39, 731 – 740.

Stockbarger D. C., "The production of Large Artificial Fluorite Crystals," *Faraday Soc*. (1949b), Disc 5, 294 – 299.

Weller P. F., J. D. Axe, G. D. Pettit, "Chemical and Optical Studies of Samarium Doped CaF2 Type Single Crystals," *J. Electrochem. Soc*. (1965), 112, 74 – 77.

Zidarova, B., "Thermoluminescence characterization of fluorites in the Slavyanka, Mikhalkovo and Ciprovtci deposits," *Compt. rend. Acad. Bulg. Sci.* (1992), 45, 8, 67 – 70.

Zidarova, B. P., "Type and distribution of the fluorite chemical inhomogeneity in Slavyanka deposit," – *Geochem. Mineral. and Petrol.* (1995), 30.

Zidarova, B. P., N. G. Zidarov, G. A. Markova, N. P. Yushkin, "Influence of natural raw material on the quality of synthetic fluorite single crystals," *Compt. rend. Acad. bulg. Sci.* (1992), 45, 3, 69 – 72.